**New Journal of Chemistry**

**Title:** A biphosphinic ruthenium complex with potent anti-bacterial and anti-cancer activity

**Authors:** José Marcos da Silveira Carvalho[a], Andressa Hellen de Morais Batista[b], Nádia Accioly Pinto Nogueira[b] , Alda Karine Medeiros Holanda[a], Jackson Rodrigues de Sousa[a], Dávila Zampieri[a], Maria Júlia Barbosa Bezerra[c], Francisco Stefânio Barreto[c] Manoel Odorico de Moraes[c], Alzir A. Batista[d], Ana Cláudia Silva Gondim[a], Tercio de F. Paulo[a], Luiz Gonzaga de França Lopes[a] , Eduardo Henrique Silva Sousa[a*]

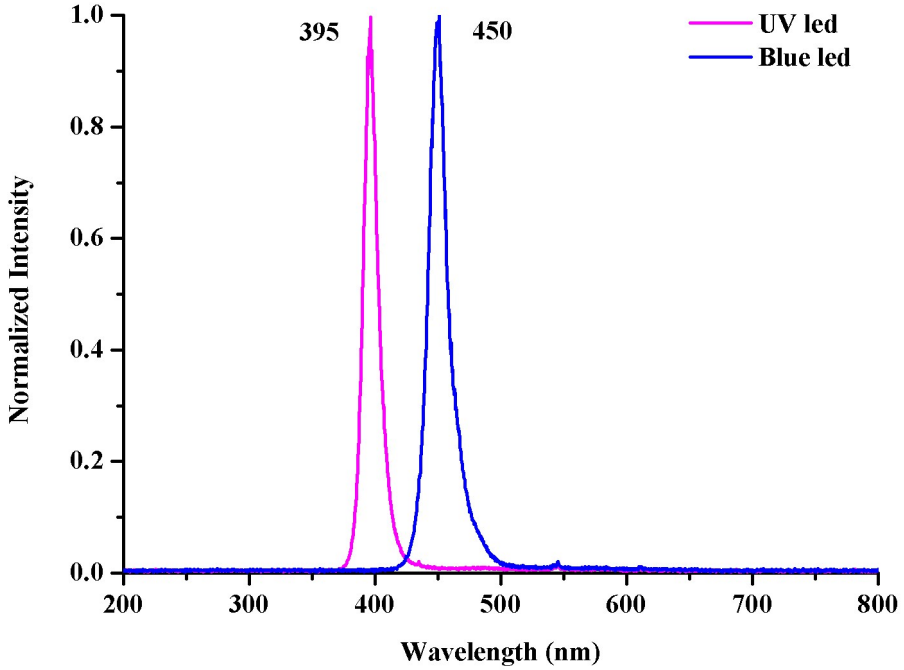


Figure S1. Spectra of the LEDs used in this paper measured using optic fiber in a spectrophotometer from Ocean Optics.

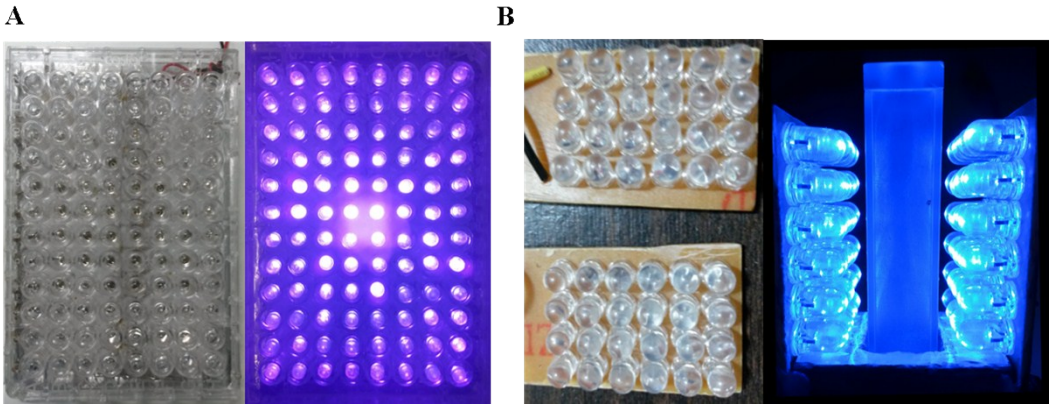


Figure S2. Home-made LEDs used in this work, microplate (A) and cuvette holder (B).

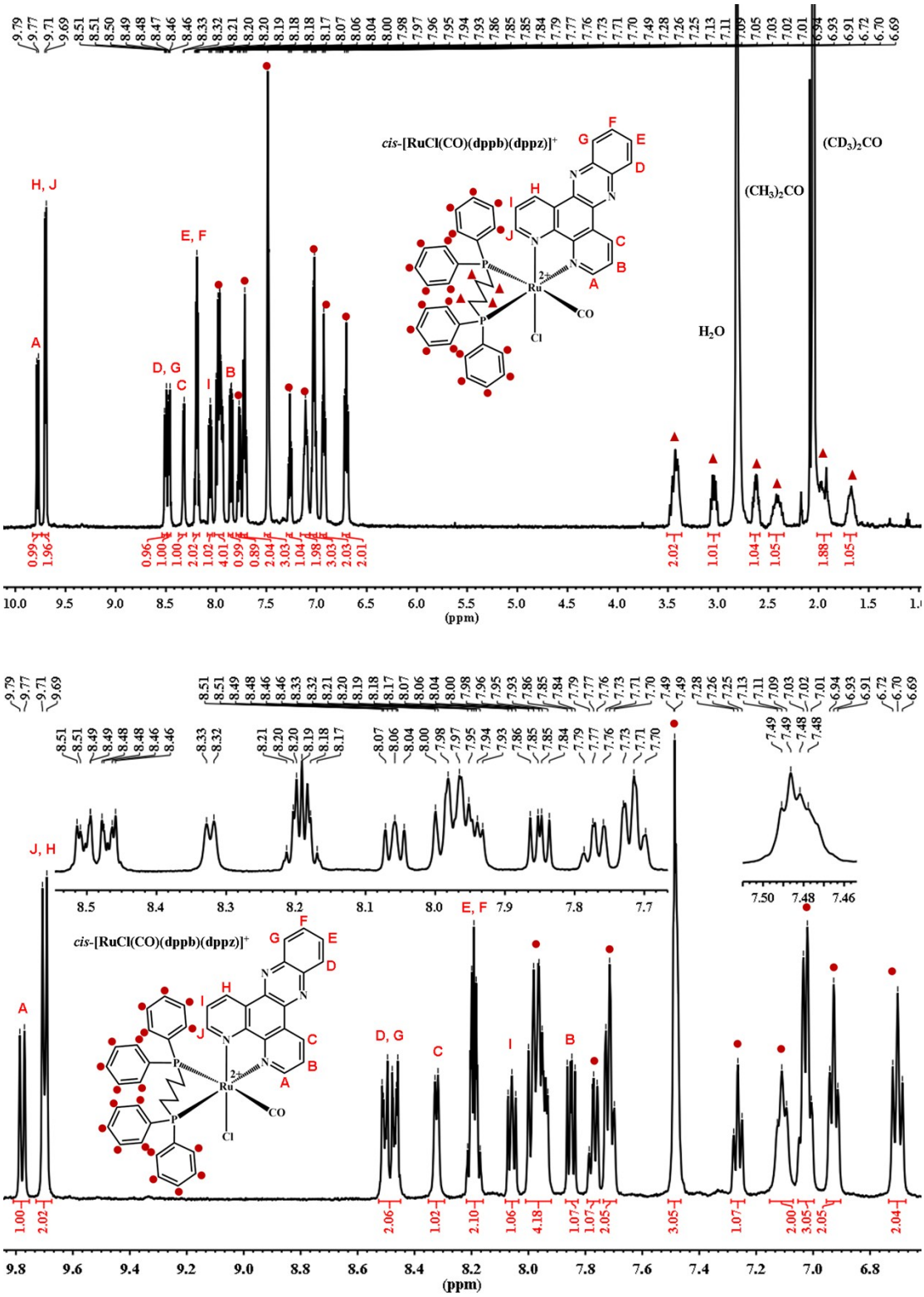


Figure S3. $^{1}$H-NMR spectrum of cis-[RuCl(dppb)(dppz)CO]$^{+}$ in $(CD_3)_2CO$ (500 MHz, 298 K). Top spectrum shows the full range of signals and the bottom spectra shows selected ranges.

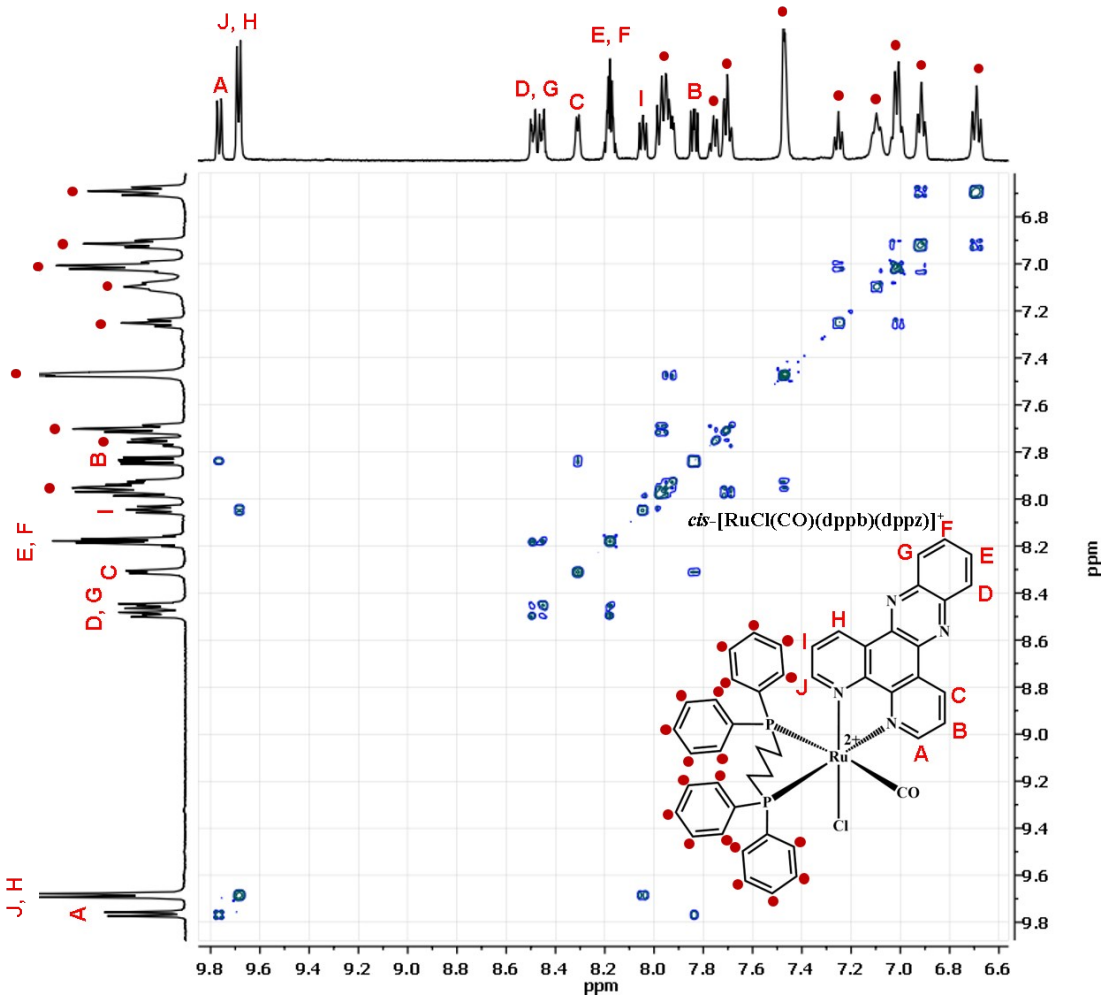


Figure S4. COSY spectrum obtained for *cis*-[Ru(CO)Cl(dppb)(dppz)]$PF_6$ in $(CD_3)_2CO$ ( 500 MHz, 298 K)

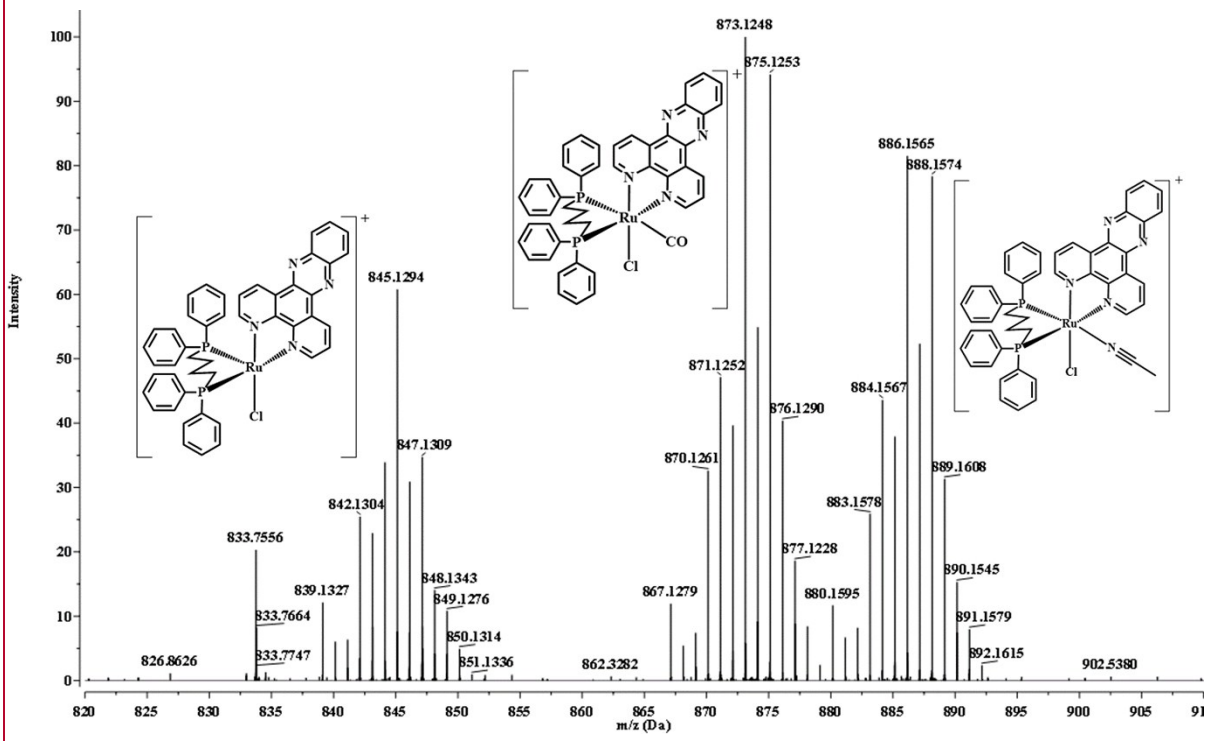


Figure S5 – High resolution mass spectrometry (ESI-TOF) for *cis*-[RuCl(CO)(dppb)(dppz)]$PF_6$ in acetonitrile.

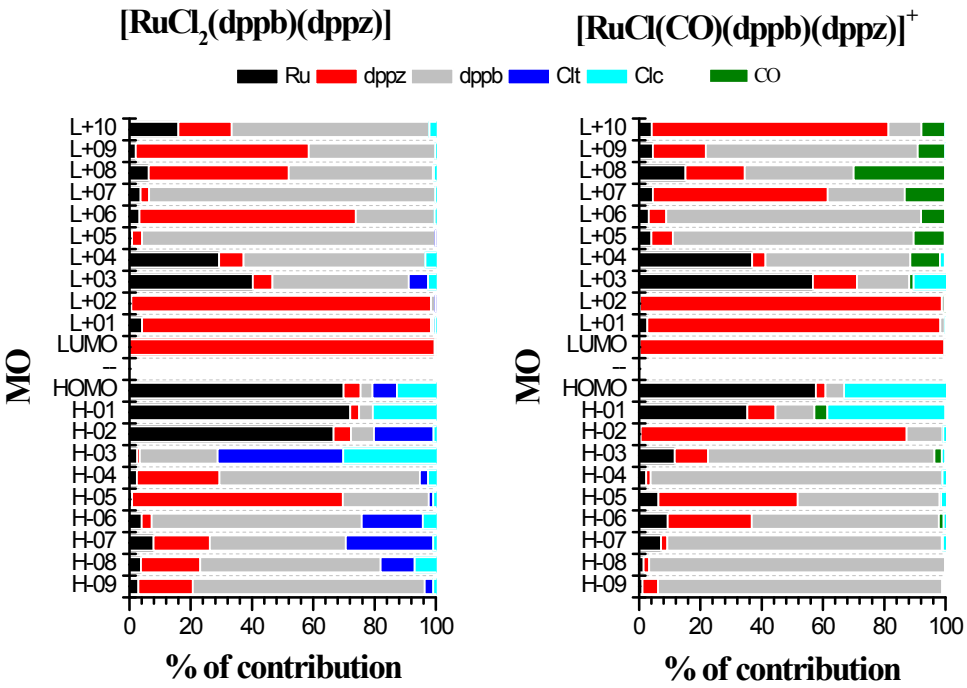


Figure S6. Percentage contribution of $Cl^-$, CO, dppb, dppz, and Ru fragments to selected frontier molecular orbitals of $[RuCl_2(dppb)(dppz)L]$ and $[RuCl(CO)(dppb)(dppz)L]^+$.

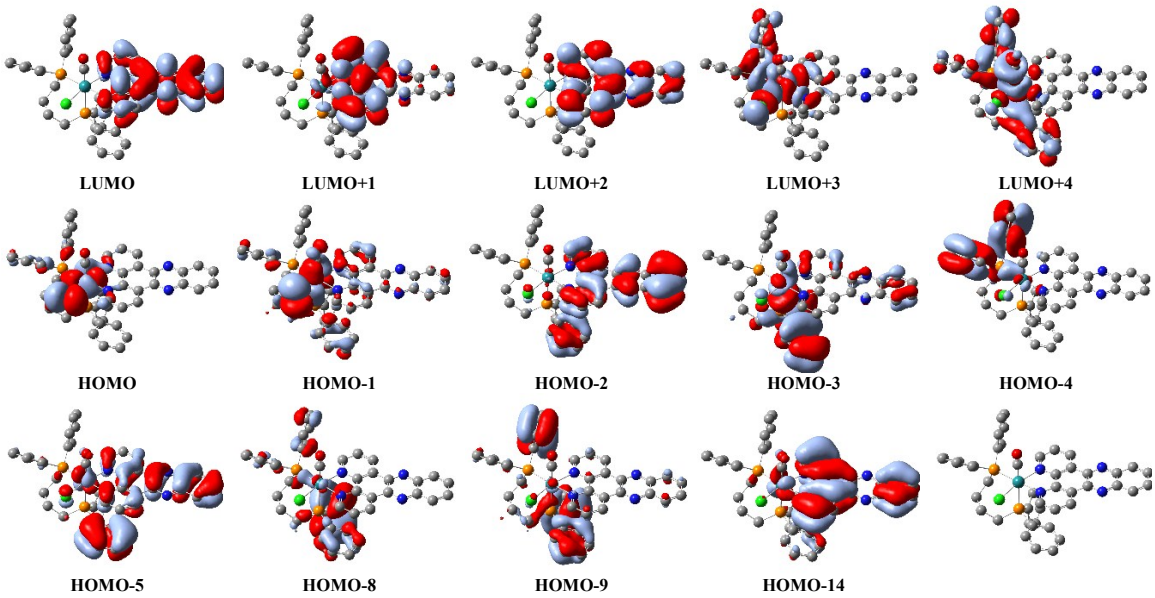


Figure S7. Select molecular orbitals for the ion complex responsible for the major UV−Vis electronic transitions by TD-DFT for cis-$[RuCl(CO)(dppb)(dppz)L]^+$.

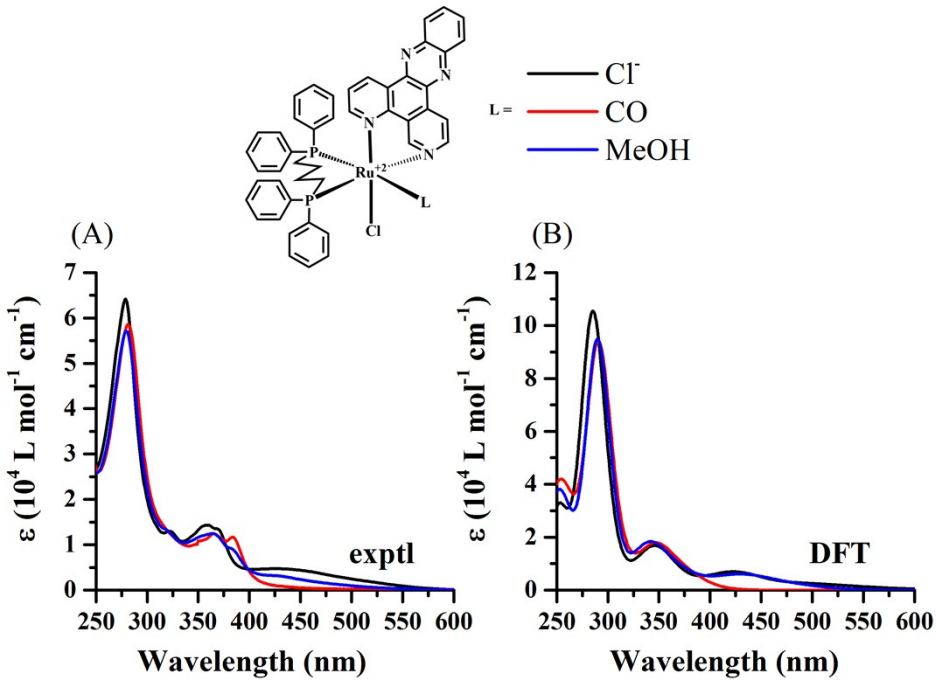


Figure S8 – Overlay of experimental (A) and simulated (B) absorption spectra of [RuCl(dppb)(dppz)L] where L= $Cl^{-}$, CO, and $CH_3OH$. A methanol polarizable continuum model was employed using the B3LYP functional and the basis sets LANL2DZ and 6-31g(d) for Ru and other atoms, respectively.

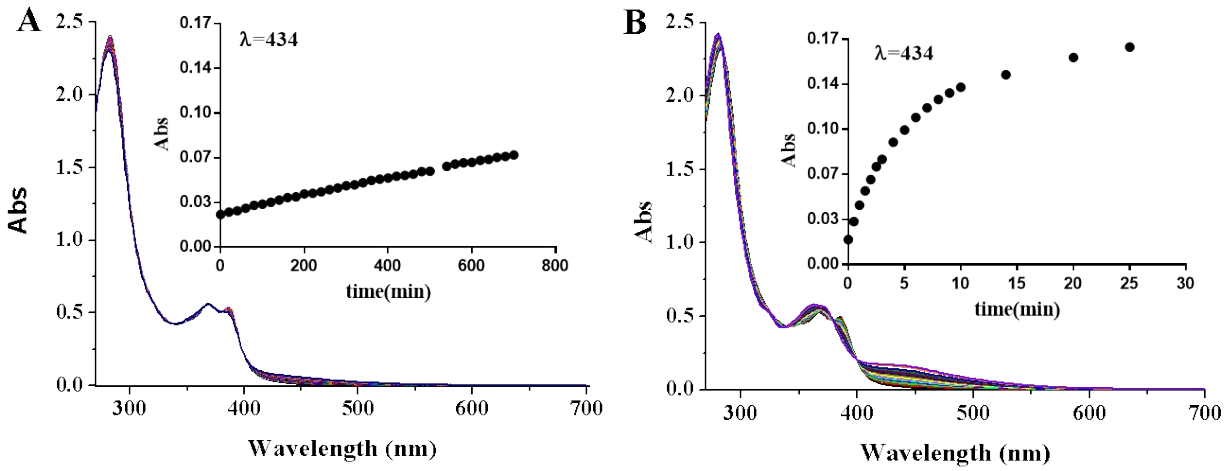


Figure S9. Monitoring spectroscopic changes of cis-[RuCl(dppb)(dppz)CO]$^{+}$ in 20% DMF:phosphate buffer pH 7.4, in the dark at 37 $^{o}$C (A) and upon blue LED irradiation at 25 $^{o}$C (B).

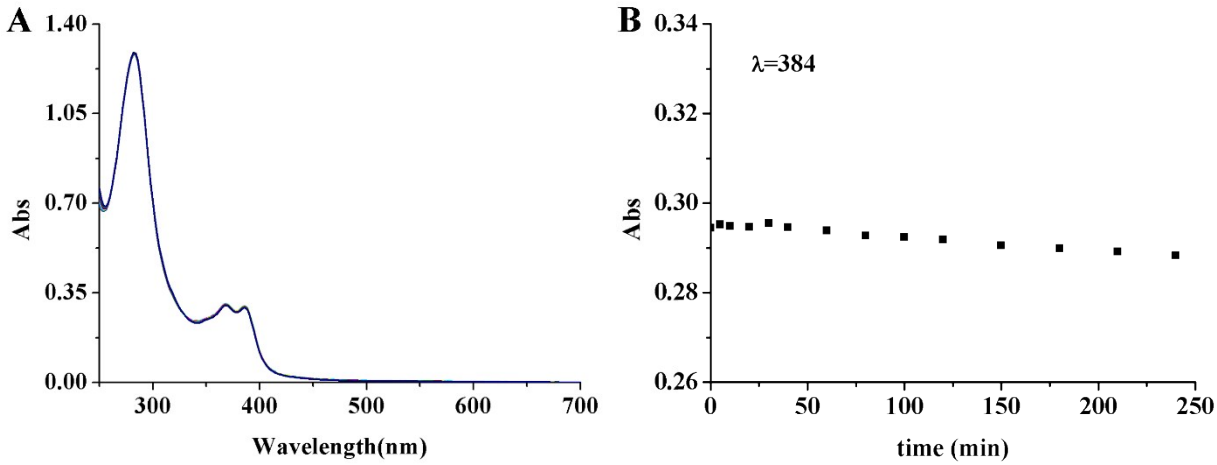


Figure S10. Reaction of glutathione (1 mmol L$^{-1}$) with cis-[RuCl(dppb)(dppz)CO]$^{+}$ (20 μmol L$^{-1}$) in 20% DMF:phosphate buffer pH 7.4 at 25 $^{o}$C monitored by UV-Vis spectroscopy. (A) shows the spectra during 4 hours and (B) the kinetic trace for changes at 384 nm.

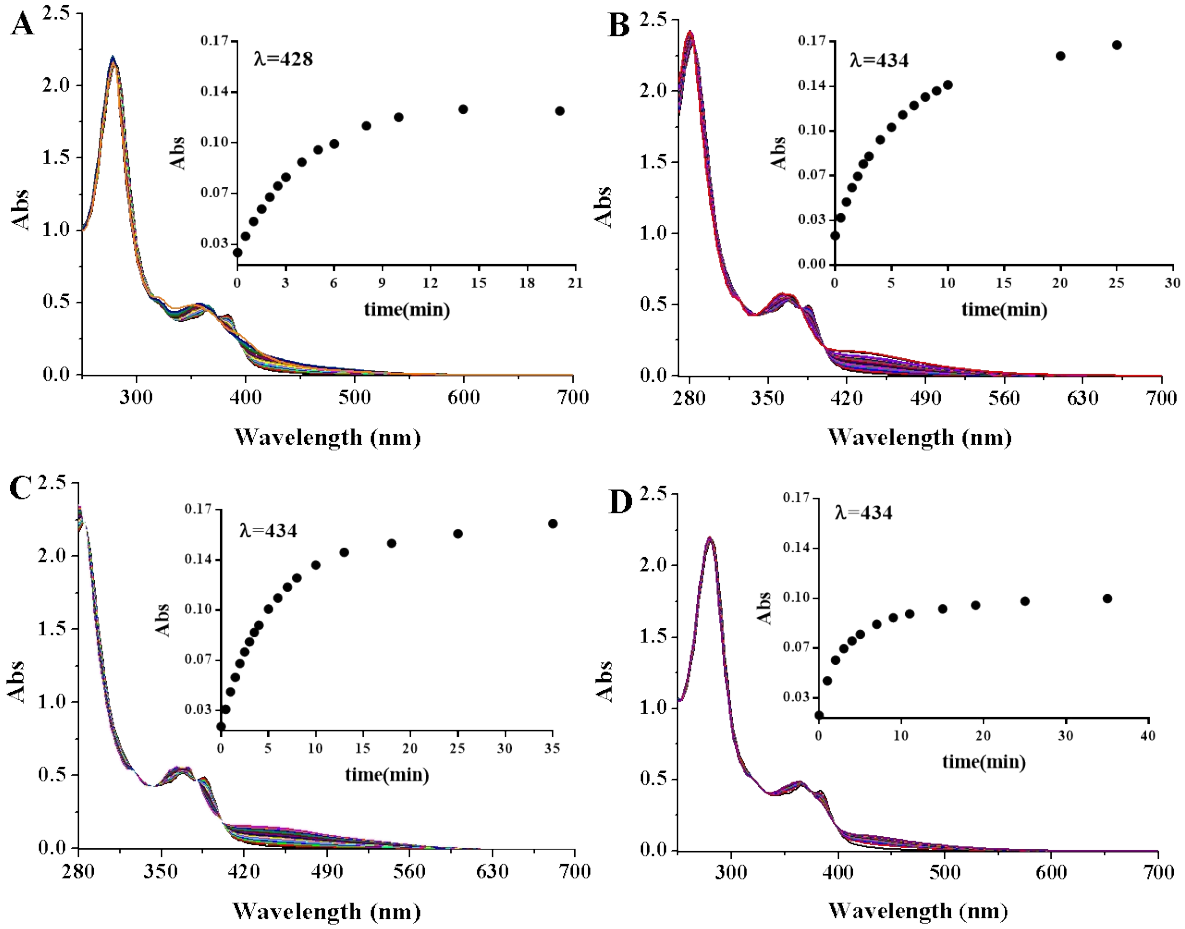


Figure S11. Spectroscopic changes of cis-[RuCl(dppb)(dppz)CO]$^{+}$ in acetonitrile (A), dimethylformamide (B), dimethylsulfoxide (C), methanol (D) upon blue LED irradiation at 25 $^{o}$C. Inset show kinetic plot during light irradiation.

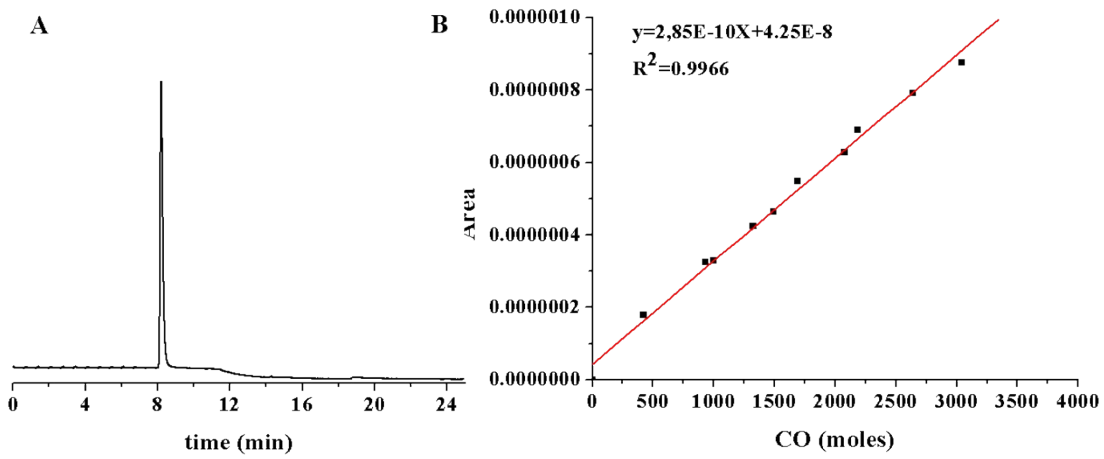


Figure S12. Gas chromatogram of the gas phase for UV irradiated sample of cis-[RuCl(CO)(dppb)(dppz)]$^{+}$ (peak with retention time at 8.20 min consistent with CO standard).

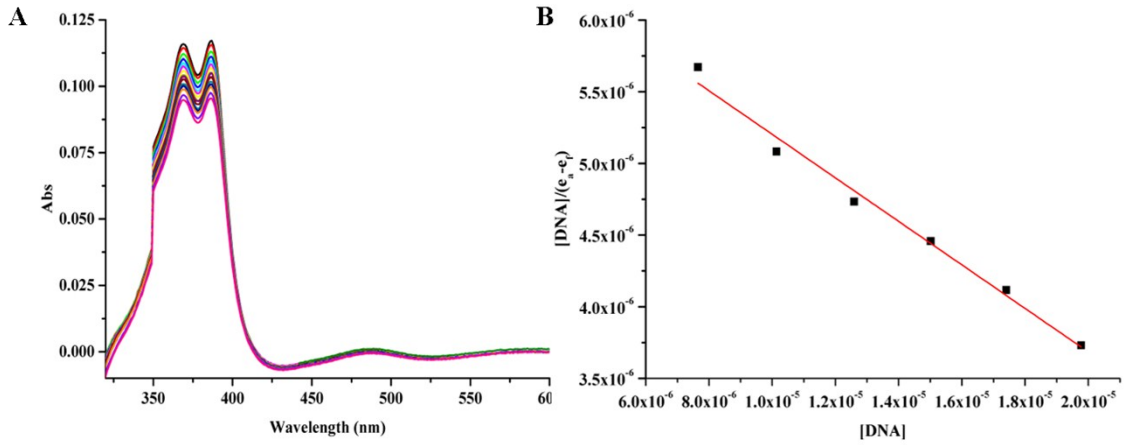


Figure S13. Calf thymus DNA (CT-DNA) titration for cis-[RuCl(CO)(dppb)(dppz)]$^{+}$ followed by electronic spectroscopy. Panel A shows spectral changes upon addition of CT-DNA and B fitting for data to obtain Kb.

**Table S1**. Selected experimental bands in the FTIR spectrum and the theoretical frequencies, ν($cm^{-1}$) and vibrational assignments of *cis*-[RuCl(CO)(dppb)(dppz)]$PF_6$.

| Experimental | DFT | Assignments |
|---|---|---|
| 518 | 498 | Ring(dppb) |
| 557 | - | β($PF_6$) |
| 518 | 537 | β(RuNO) |
| 696 | 690 | Ring(dppb) |
| 836 | - | ν($PF_6$) |
| 1077 | 1072 | β(CH) |
| 1357 | 1347 | ν(CC), ν(CN) dppz |
| 1434 | 1433 | β(CH) dppb |
| 1492 | 1492 | ν(CC), ν(CN) dppz |
| 1993 | 2023 | ν(CO) |

Table S2. Selected UV−Vis Energy Transitions at the TD-DFT/B3LYP Level for *cis*-[RuCl(CO)(dppb)(dppz)]$^{+}$ in acetonitrile.

| $\lambda_{cal.}$ (nm) | Oscillator strength (*f*) | Key transition | Character |
|---|---|---|---|
| 379 | 0.0485 | H-1→LUMO (79%) | $d_{Ru}/\pi_{Cl} \rightarrow \pi^*_{dppz}$ |
| 370 | 0.0178 | H-2 → LUMO (92%) | $\pi_{dppz} \rightarrow \pi^*_{dppz}$ |
| 361 | 0.0218 | H-3 → LUMO (88%) | $\pi_{dppb}/d_{Ru} \rightarrow \pi^*_{dppz}$ |
| 346 | 0.1766 | H-5→LUMO (62%) | $\pi_{dppz}/\pi_{dppb}/d_{Ru} \rightarrow \pi^*_{dppz}$ |
| 294 | 0.3054 | H-8→L+1 (19%)<br>H-2→L+2 (24%) | $\pi_{dppb} \rightarrow \pi^*_{dppz}$<br>$\pi_{dppz} \rightarrow \pi^*_{dppz}$ |
| 291 | 0.4327 | H-9→L+1 (35%) | $\pi_{dppb} \rightarrow \pi^*_{dppz}$ |
| 287 | 0.2184 | H-5→L+2 (66%) | $\pi_{dppz}/\pi_{dppb}/d_{Ru} \rightarrow \pi^*_{dppz}$ |
| 262 | 0.1764 | H-14→L+1 (42%) | $\pi_{dppz} \rightarrow \pi^*_{dppz}$ |
| 253 | 0.1963 | H-3→L+4 (38%) | $\pi_{dppb}/d_{Ru} \rightarrow d_{Ru}/\pi_{dppb}/\pi_{CO}$ |

Table S3. Half-life for photolysis of the *cis*-[RuCl(CO)(dppb)(dppz)]$^{+}$ using blue LED in different solvents and mixtures at 25 ºC.

| **Solvent** | **$t_{1/2}$ (min)** |
|---|---|
| DMF | 3.88 |
| Methanol | 2.36 |
| DMSO | 3.76 |
| Acetonitrile | 2.87 |
| PBS/DMF | 3.82 |
| PBS/DMF-dark | 1157.95 |